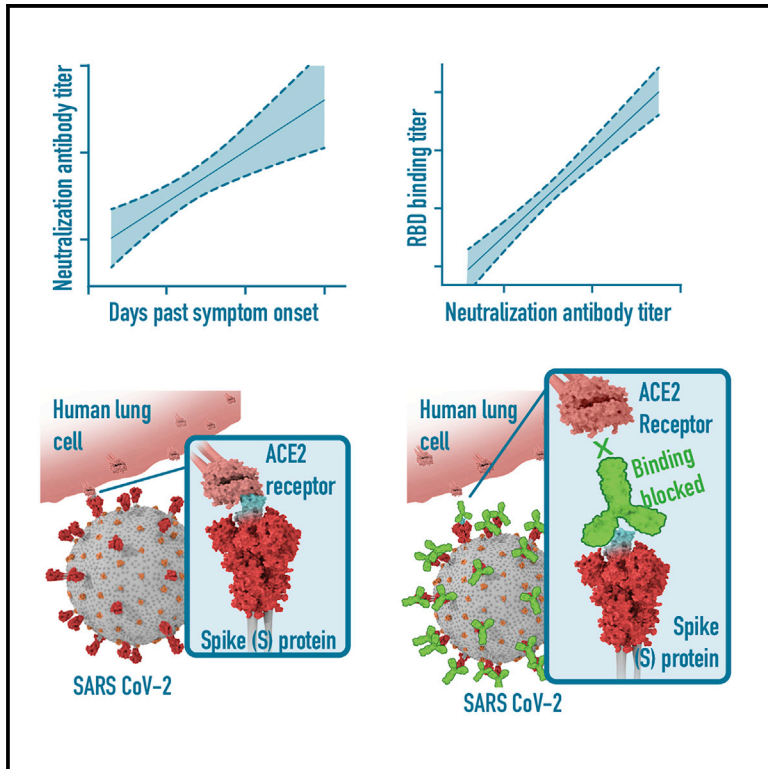


# Rapid Generation of Neutralizing Antibody Responses in COVID-19 Patients

## Graphical Abstract



## Authors

Mehul S. Suthar, Matthew G. Zimmerman, Robert C. Kauffman, ..., Rafi Ahmed, John D. Roback, Jens Wrammert

## Correspondence

mehul.s.suthar@emory.edu (M.S.S.), jwramme@emory.edu (J.W.)

## In Brief

Suthar et al. report on a cross-sectional study of hospitalized COVID-19 patients suggesting a correlation between the SARS-CoV-2 receptor-binding-domain-specific IgG responses and virus neutralizing antibody responses. These findings have implications for understanding protective immunity against SARS-CoV-2, therapeutic use of immune plasma, and development of vaccines.

## HIGHLIGHTS

- Cross-sectional study of 44 hospitalized COVID-19 patients
- RBD-specific IgG responses detectable in all patients 6 days after PCR confirmation
- Neutralizing titers are detectable in all patients 6 days after PCR confirmation
- RBD-specific IgG titers correlate with the neutralizing potency



## Article

# Rapid Generation of Neutralizing Antibody Responses in COVID-19 Patients

Mehul S. Suthar,<sup>1,2,3,12,\*</sup> Matthew G. Zimmerman,<sup>1,2,3,11</sup> Robert C. Kauffman,<sup>1,2,11</sup> Grace Mantus,<sup>1,2,11</sup> Susanne L. Linderman,<sup>2,4</sup> William H. Hudson,<sup>2,4</sup> Abigail Vanderheiden,<sup>1,2,3</sup> Lindsay Nyhoff,<sup>1,2</sup> Carl W. Davis,<sup>2,4</sup> Oluwaseyi Adekunle,<sup>1,2</sup> Maurizio Affer,<sup>1,2</sup> Melanie Sherman,<sup>5</sup> Stacian Reynolds,<sup>5</sup> Hans P. Verkerke,<sup>6</sup> David N. Alter,<sup>6</sup> Jeannette Guarner,<sup>6</sup> Janetta Bryksin,<sup>6</sup> Michael C. Horwath,<sup>6</sup> Connie M. Arthur,<sup>6</sup> Natia Saakadze,<sup>6</sup> Geoffrey H. Smith,<sup>6</sup> Srilatha Edupuganti,<sup>7,8</sup> Erin M. Scherer,<sup>7,8</sup> Kieffer Hellmeister,<sup>7,8</sup> Andrew Cheng,<sup>7,8</sup> Juliet A. Morales,<sup>7,8</sup> Andrew S. Neish,<sup>6</sup> Sean R. Stowell,<sup>6</sup> Philipp Frank,<sup>9</sup> Eric Ortlund,<sup>9</sup> Evan J. Anderson,<sup>1</sup> Vineet D. Menachery,<sup>10</sup> Nadine Roupheal,<sup>7,8</sup> Aneesh K. Mehta,<sup>8</sup> David S. Stephens,<sup>8</sup> Rafi Ahmed,<sup>2,4</sup> John D. Roback,<sup>6</sup> and Jens Wrangøe<sup>1,2,\*</sup>

<sup>1</sup>Center for Childhood Infections and Vaccines; Children's Healthcare of Atlanta and Emory University Department of Pediatrics, Atlanta, GA 30322, USA

<sup>2</sup>Emory Vaccine Center, Emory University School of Medicine, Atlanta, GA 30329, USA

<sup>3</sup>Yerkes National Primate Research Center, Atlanta, GA 30329, USA

<sup>4</sup>Department of Microbiology and Immunology, Emory University School of Medicine, Atlanta, GA 30322, USA

<sup>5</sup>Emory Medical Laboratories, Emory Healthcare, Atlanta, GA 30322, USA

<sup>6</sup>Department of Pathology and Laboratory Medicine, Emory University School of Medicine, Atlanta, GA 30322, USA

<sup>7</sup>Hope Clinic of the Emory Vaccine Center, Emory University School of Medicine Decatur, Atlanta, GA, USA

<sup>8</sup>Division of Infectious Diseases, Department of Medicine, Emory University School of Medicine, Atlanta, GA, USA

<sup>9</sup>Department of Biochemistry, Emory University School of Medicine, Atlanta, GA, USA

<sup>10</sup>Department of Microbiology and Immunology, Institute for Human Infection and Immunity, World Reference Center for Emerging Viruses and Arboviruses, University of Texas Medical Branch, Galveston, TX, USA

<sup>11</sup>These authors contributed equally

<sup>12</sup>Lead Contact

\*Correspondence: [mehul.s.suthar@emory.edu](mailto:mehul.s.suthar@emory.edu) (M.S.S.), [jwramme@emory.edu](mailto:jwramme@emory.edu) (J.W.)

<https://doi.org/10.1016/j.xcrm.2020.100040>

## SUMMARY

SARS-CoV-2, the virus responsible for COVID-19, is causing a devastating worldwide pandemic, and there is a pressing need to understand the development, specificity, and neutralizing potency of humoral immune responses during acute infection. We report a cross-sectional study of antibody responses to the receptor-binding domain (RBD) of the spike protein and virus neutralization activity in a cohort of 44 hospitalized COVID-19 patients. RBD-specific IgG responses are detectable in all patients 6 days after PCR confirmation. Isotype switching to IgG occurs rapidly, primarily to IgG1 and IgG3. Using a clinical SARS-CoV-2 isolate, neutralizing antibody titers are detectable in all patients by 6 days after PCR confirmation and correlate with RBD-specific binding IgG titers. The RBD-specific binding data were further validated in a clinical setting with 231 PCR-confirmed COVID-19 patient samples. These findings have implications for understanding protective immunity against SARS-CoV-2, therapeutic use of immune plasma, and development of much-needed vaccines.

## INTRODUCTION

Coronavirus disease 2019 (COVID-19) is a worldwide pandemic. There is a pressing need to understand the immunological response that mediates protective immunity to SARS-CoV-2. Antibody responses to the spike (S) protein are thought to be to the primary target of neutralizing activity during viral infection, conferring superior protective immunity compared to the membrane (M), envelope (E), and nucleocapsid proteins.<sup>1-3</sup> The S glycoprotein is a class I viral fusion protein that exists as a metastable prefusion homotrimer consisting of individual polypeptide chains (between 1,100 and 1,600 residues in length) responsible for cell attachment and viral fusion.<sup>4-6</sup> Each of the S protein pro-

tomers is divided into two distinct regions, the S<sub>1</sub> and S<sub>2</sub> subunits.<sup>4,7</sup> The S<sub>1</sub> subunit is a V-shaped polypeptide with four distinct domains, domains A, B, C, and D, with domain B functioning as the receptor-binding domain (RBD) for most coronaviruses, including the pathogenic  $\beta$ -coronaviruses such as SARS-CoV-2, severe acute respiratory syndrome (SARS), and Middle East respiratory syndrome (MERS) (Figure 1A; Figure S1A).<sup>7-10</sup> Recent studies have shown that the SARS-CoV-2 RBD interacts with the ACE2 receptor for cellular attachment.<sup>5,6,10</sup> Sequence analysis of the RBD shows extensive homology in this region to SARS (73%). In contrast, MERS and other seasonal coronaviruses show minimal sequence homology to the SARS-CoV-2 RBD (7%–18%) (Figure 1B). Herein, we set out to understand



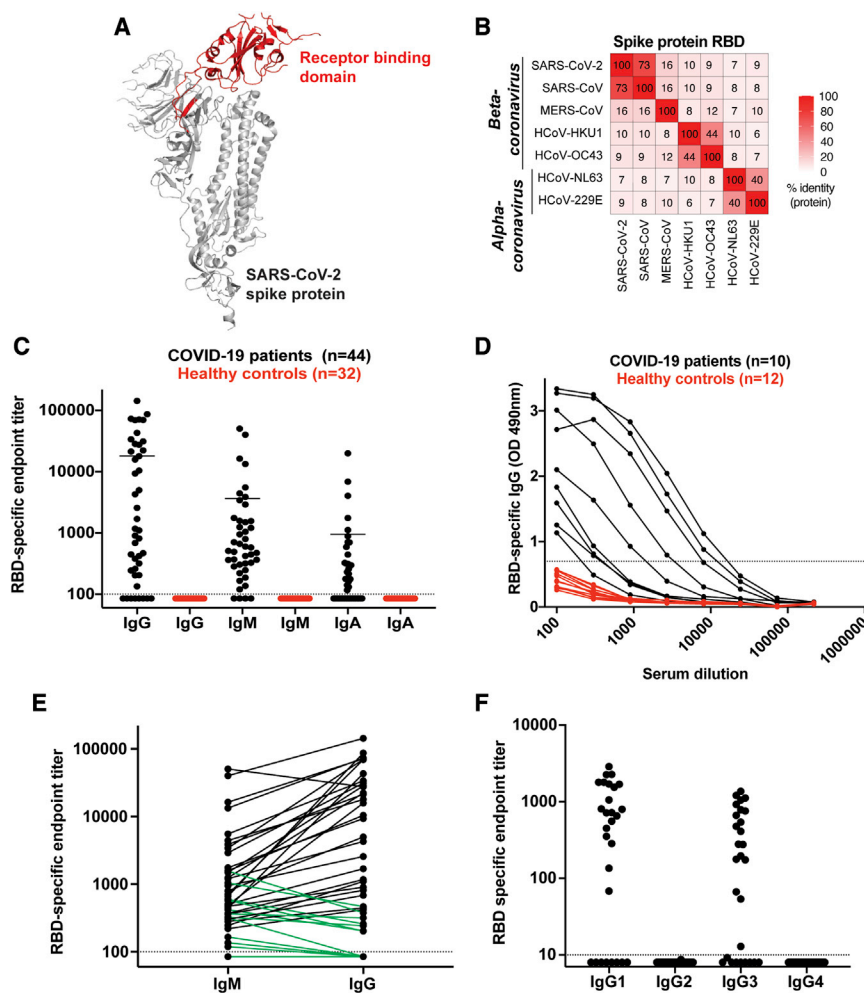


**Figure 1. Antibody Responses against SARS-CoV-2 RBD in PCR-Confirmed Acutely Infected COVID-19 Patients**

(A) Structure of a SARS-CoV-2 spike protein (single monomer is shown) with the RBD highlighted in red.<sup>5</sup>

(B) Sequence homology analysis of SARS-CoV-2 spike protein RBD compared to SARS, MERS, and seasonal alpha- and beta-CoVs.

(C) ELISA endpoint titers for SARS-CoV-2 RBD-specific IgG, IgA, and IgM in PCR confirmed acute COVID-19 patients (n = 44) and healthy controls collected in early 2019. Endpoint cutoff values were calculated using the average plus 3 standard deviations of the 32 healthy controls at 1/100 dilution (shown as a dotted line).

(D) Representative ELISA assays for 10 patients and 12 healthy controls.

(E) Direct comparison of IgM and IgG for individual donors. A number of the IgG negative or low early samples were IgM positive (shown in green).

(F) Endpoint titer analysis of IgG subclass distribution. Each experiment was performed at least twice, and representative donors were selected to display the dynamic range observed in the dataset.

the development, specificity, and neutralizing potency of the humoral immune response against the RBD of the SARS-CoV-2 spike protein during acute infection.

## RESULTS

### The Magnitude of RBD-Specific Antibody Responses in Acutely Infected COVID-19 Patients

To determine the magnitude of antibody responses, immunoglobulin (Ig) isotype, and IgG subclass usage against the RBD of the SARS-CoV-2 spike protein, we analyzed a cohort of acutely infected COVID-19 patients (n = 44) enrolled at two hospitals in the Emory Healthcare System in Atlanta (Emory University Hospital and Emory University Hospital Midtown). These patients were recruited from both the inpatient ward and the ICU (patient details are provided in Table 1). These samples represent a cross-section of days after patient-reported symptom onset (3–30 days) and PCR confirmation (2–19 days). As healthy controls, we used plasma samples collected at baseline in a vaccine study performed in early 2019 (n = 32). The RBD protein was cloned and expressed in mammalian cells (Figure S1B) and was validated by ELISA using CR3022, a SARS-specific human

monoclonal antibody that cross-reacts with SARS-CoV-2<sup>11</sup> (Figure S1C). Size-exclusion chromatography shows that the recombinant RBD protein is homogeneous and does not form aggregates (Figure S1D). We found that a majority of COVID-19 patients (36 out of 44) developed RBD-specific class-switched IgG responses (Figure 1C) (mean titer: 18,500, range: <100–142,765). These patients also showed IgM and IgA responses of lower magnitude as compared to IgG (IgM mean titer: 3731, range: <100–40,197 and IgA mean titer: 973, range: <100–19,918). All of the negative controls were below the limit of detection in the endpoint analysis for binding to the RBD antigen (Figure 1C, red). A representative RBD-specific IgG ELISA assay for a subset of these donors is shown in Figure 1D to illustrate the dynamic range of these measurements. A number of the COVID-19 patient samples that scored either negative or low in the RBD IgG ELISA had higher titers of IgM (Figure 1E, green). Finally, IgG subclass analysis showed that the COVID-19 patients exclusively made RBD-specific IgG1 and IgG3, with no detectable IgG2 or IgG4 (Figure 1F). Taken together, these findings illustrate that antibody class-switching to IgG occurs early during acute infection.

### Neutralization Potency of Antibody Responses in COVID-19 Patients

We next determined the neutralization capacity of samples from the cohort of acutely infected COVID-19 patients. We have developed a focus reduction neutralization titer (FRNT) assay for SARS-CoV-2. In this assay, COVID-19 patient plasma is incubated with a clinical isolate of SARS-CoV-2 followed by infection

**Table 1. COVID-19 Patient Cohort**

Patient ID#	Age	Sex	Days after +PCR	Days after Symptom Onset	IgG	IgM	IgA	FRNT50
1	25	F	2	3	<100	<100	<100	<50
2	41	M	2	8	259	599	116	245
3	66	M	2	10	4,988	795	297	1,502
4	76	F	2	11	31,205	2906	230	1,718
5	70	F	2	11	1,100	246	<100	138
6	74	M	2	12	<100	<100	<100	<50
7	33	F	3	7	243	325	<100	174
8	66	M	3	8	419	220	85	167
9	64	F	3	8	<100	166	<100	55
10	39	F	3	8	814	362	287	262
11	87	M	3	9	<100	<100	<100	124
12	64	F	3	9	<100	119	161	67
13	47	F	3	9	467	1,042	<100	158
14	63	F	3	10	134	186	<100	99
15	58	F	3	11	317	364	258	175
16	37	F	3	13	205	419	<100	126
17	37	F	3	14	202	578	<100	118
18	49	M	3	16	15,772	491	589	126
19	70	M	4	5	<100	136	<100	156
20	55	M	4	8	377	1,560	178	79
21	73	M	4	11	683	303	<100	<50
22	61	M	4	19	445	282	<100	645
23	80	M	5	5	899	470	316	167
24	44	F	5	9	2,560	947	442	194
25	63	F	5	12	<100	<100	<100	<50
26	52	M	5	12	<100	317	<100	108
27	56	M	5	17	10,422	1,574	4,033	3,200
28	48	M	6	8	9,311	1,750	884	1,068
29	60	M	6	10	27,557	50,483	<100	5,763
30	75	M	6	18	1,174	369	131	539
31	59	M	7	11	21,323	3,865	140	2,799
32	62	F	7	12	17,917	4,414	706	603
33	76	M	7	17	28,352	1,493	6,865	2,561
34	66	M	7	22	4,269	1,207	324	496
35	80	M	7	29	22,219	1,242	176	2,483
36	65	M	8	8	1,692	507	<100	761
37	36	F	8	15	86,698	664	313	2,233
38	60	F	8	15	43,072	443	214	337
39	56	F	8	18	71,204	16,298	1,754	1,177
40	54	M	10	30	72,949	13,310	700	3,341
41	60	M	12	17	142,766	40,197	<100	5,378
42	46	M	13	20	69,361	706	1,112	408
43	73	M	15	11	69,902	3,412	19,918	911
44	69	M	19	18	33,684	5,517	180	1,882

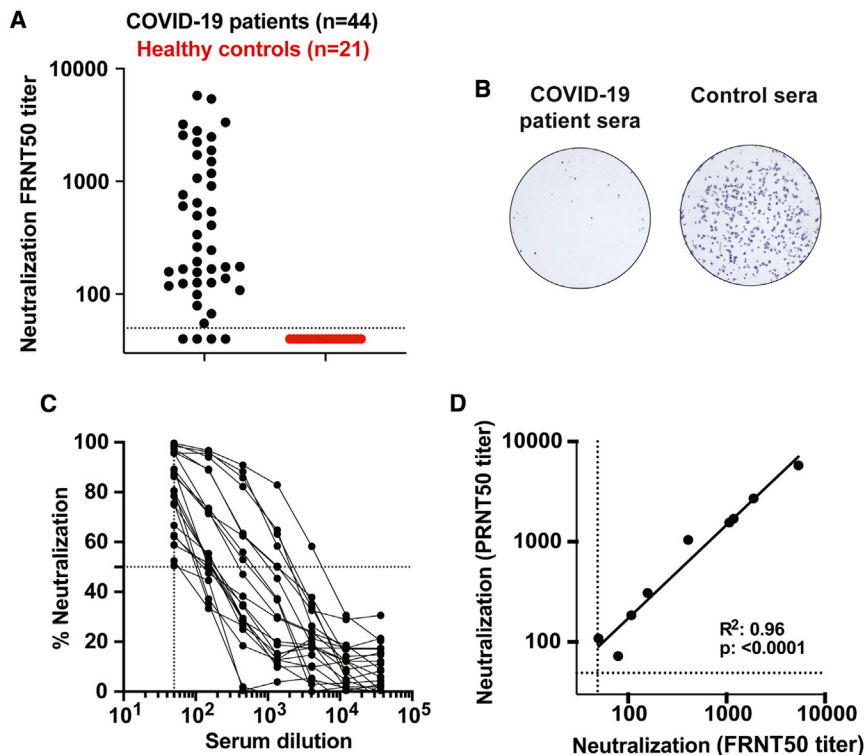


**Figure 2. COVID-19 Patient Plasma Neutralizes SARS-CoV-2**

(A) Neutralization activity of serum samples against SARS-CoV-2. The FRNT<sub>50</sub> titers of COVID-19 patients (n = 44) and healthy controls (n = 21) sera were determined by a FRNT assay using an immunostain to detect infected foci. Each circle represents one serum sample. The dotted line represents the maximum concentrations of the serum tested (1/50).

(B) Representative sample showing a reduction in foci from a neutralization assay with sera from an infected COVID-19 patient.

(C) Representative FRNT<sub>50</sub> curves were selected to display the dynamic range observed in the dataset (n = 22). The dotted line represents 50% neutralization.

(D) Comparison of PRNT<sub>50</sub> against FRNT<sub>50</sub> titers (n = 9). Each experiment was performed at least twice, and a representative dataset is shown.

of VeroE6 cells.<sup>12</sup> The neutralization potency of the plasma sample is measured by the reduction in virally infected foci. We screened plasma from COVID-19 patients (n = 44) and found that a majority of the samples (40/44) showed neutralization capacity, with titers ranging from 1:5,763 to 1:55 (Figure 2A). A representative example of viral neutralization is shown in Figure 2B where pre-incubation with control plasma yields about 250 foci, whereas the COVID-19 patient sample completely inhibited the formation of infected foci (Figure 2B). Representative neutralization curves for a subset of samples are shown to illustrate the dynamic range of the results obtained (Figure 2C). A plaque reduction neutralization titer (PRNT) assay is the classic method for determining the neutralization capacity of a plasma sample against coronavirus infection.<sup>13</sup> To confirm the efficiency of these two assays, we compared the neutralization titers between a standard PRNT assay and an FRNT assay for a subset of the patient samples (n = 9). Overall, we observed a strong positive correlation between these two assays (Figure 2D), demonstrating the robustness of the FRNT assay. Overall, these findings demonstrate that neutralizing antibody responses are generated early during acute COVID-19 infection.

#### Development of Antibody Responses during Acute SARS-CoV-2 Infection

The patient samples were collected across a range of days after symptom onset or PCR confirmation of SARS-CoV-2 infection (Table 1). To understand the relationship between these variables and RBD-specific IgG antibody titers and viral neutralization potency, we performed correlation analyses. In all cases,

we observed significant correlations between the number of days elapsed after symptom onset or positive PCR test and the RBD-specific IgG titer or viral neutralization titer (Figure 3). Several key points regarding the kinetics of antibody responses can be made from this correlation analysis. Antibody responses against the RBD (Figure 3A), as well as SARS-CoV-2 virus neutralization titers (Figure 3B), can be detected in a majority of patients around day 8 after symptom onset. When the number of days after PCR confirmation is used to assess the duration of infection, both RBD-binding titers (Figure 3C) and viral neutralization titers (Figure 3D) can be detected in many patients already between days 2–6. Beyond 6 days post-PCR confirmation, patients display both antibody binding and neutralization titers. Taken together, these findings illustrate that both RBD-specific and neutralizing antibody responses occur rapidly after SARS-CoV-2 infection.

#### RBD-Specific Antibody Titers as a Surrogate of Neutralization Potency in Acutely Infected COVID-19 Patients

We observed a wide range of RBD-specific and neutralizing antibody responses across the cohort of acutely infected COVID-19 patients. We found that the magnitude of RBD-specific IgG titers positively correlated with neutralization titers ( $r^2 = 0.7$ ;  $p < 0.0001$ ; Figure 4A). Overall, we observed viral neutralization activity in 40 out of 44 samples from acutely infected COVID-19 patients.

We next validated the RBD-specific IgG ELISA for high-throughput testing at the Emory Medical Laboratories. For these analyses, we collected serum from 231 PCR-confirmed COVID-19 patient samples within the first 22 days after PCR confirmation (Table S1). In addition, 490 samples collected in 2019 were used as negative controls. The patient samples were grouped from 0–3 days, 4–6 days, and 7 or more days after PCR confirmation and analyzed using a high-throughput clinical RBD ELISA. The cumulative results of these efforts are shown as

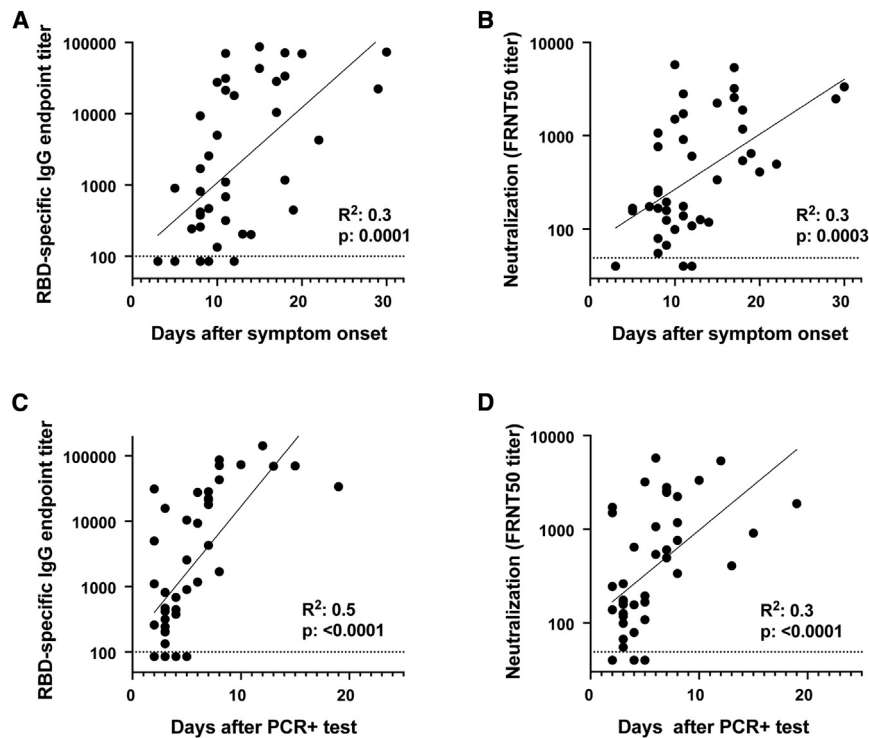


**Figure 3. SARS-CoV-2 Antibody Responses Correlate with the Progression of Acute SARS-CoV-2 Infection**

Comparison of RBD-specific IgG titers and neutralization titers with (A and B) days after symptom onset or (C and D) days after PCR positive confirmation for each patient. Correlation analysis was performed by log transformation of the endpoint ELISA titers followed by linear regression analysis.

findings demonstrate that RBD-specific IgG titers could be used as a surrogate of neutralization activity against SARS-CoV-2 infection and that the RBD assay is highly specific and sensitive. Further, this demonstrates the necessity of appropriate timing of sample collection when using serologic diagnostic tests of acutely infected COVID-19 patients.<sup>14,15</sup>

## DISCUSSION

In this study, we show that RBD-specific IgG antibody responses are rapidly induced in hospitalized acutely infected COVID-19 patients, with most patients

receiver operating characteristic (ROC) curves (Figure 4B). This assay is almost perfectly discriminatory by day 7 after PCR confirmation, with an area under the curve (AUC) of 1.00 (n = 83). When utilized earlier in the disease course, the performance of this diagnostic assay is reduced. When the RBD-specific IgG ELISA were analyzed for the samples collected closer to the time of infection, the AUC for the day 4–6 group (n = 76) and the day 0–3 group (n = 72) fell to 0.96 and 0.89, respectively. Using an OD cutoff of 0.175 resulted in calculated sensitivity and specificity values of 97.5% and 98%, respectively. Taken together, these

showing RBD-specific antibody responses by 6 days post-PCR confirmation. Consistently, we found that class-switching also occurs early during infection and is dominated by RBD-specific IgG1 and IgG3 responses. We also detected both RBD-specific IgM and IgA responses at relatively lower levels as compared to IgG. These responses result in neutralizing antibody responses that directly correlated with RBD-specific IgG antibody titers. These findings strongly indicate that a robust humoral immune response occurs early during severe or moderate COVID-19 infections.

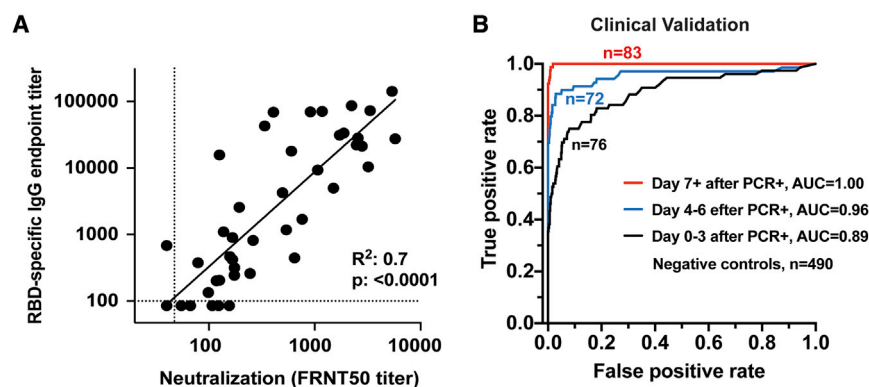


**Figure 4. RBD-Specific Antibody Titers as a Surrogate of Neutralization Potency in Acutely Infected COVID-19 Patients**

(A) Comparison of RBD-specific IgG endpoint titers with SARS-CoV-2-specific FRNT<sub>50</sub> titers. Correlation analysis was performed by log transformation of the endpoint ELISA or FRNT<sub>50</sub> titers followed by linear regression analysis.

(B) The RBD-specific ELISA was validated for high-throughput clinical testing in Emory Medical Laboratories. Sera (n = 231) were collected from COVID-19 patients within the first 22 days after PCR-confirmation (Table S1). Sera (n = 490) collected in 2019 were used as negative controls. ROC curves are shown comparing the true-positive and false-negative rates of the ELISA using different OD cutoffs and sera collected at different

times post-infection. Whereas the RBD ELISA produced an area under the curve (AUC) of 0.89 when samples were collected close to the time of infection (within 3 days of positive PCR; n = 76), longer sampling times resulted in better performance. Assay performance was nearly perfectly discriminatory (AUC = 1.00) when samples were collected at least 7 days after the positive PCR (n = 83).

The validation of the sensitive and selective RBD-based clinical assay at Emory Medical Laboratories and the correlation with viral neutralization are promising for both diagnostic purposes and ongoing seroprevalence studies of healthcare workers and the general population. These serology tests could be used for making informed decisions for convalescent plasma therapy that are currently undergoing clinical testing as a possible therapeutic or even prophylactic option.<sup>16,17</sup> Further, the kinetic findings presented herein are essential for ongoing efforts aimed at applying antibody testing for clinical diagnostic purposes, highlighting the importance of appropriate timing of these tests relative to PCR testing and/or symptom onset after infection. A comprehensive understanding of the dynamics of antibody responses after infection will also be key for understanding disease pathogenesis, risk assessment in vulnerable populations, evaluation of therapeutics, and development of vaccines.

The appearance of high titer neutralizing antibody responses early after the infection is promising and may offer some degree of protection from re-infection. Future studies will need to define the neutralizing titer that constitutes a robust correlate of protective immunity and determine the durability of these responses over time<sup>18</sup>. This information will be essential for ongoing vaccine development efforts<sup>19</sup>.

### Limitations of Study

This report is a cross-sectional study that analyzed antibody responses to SARS-CoV-2 in a cohort of hospitalized COVID-19 patients. One limitation is that this study only includes patients with severe disease. In the future, we will extend these observations to evaluate antibody responses in patients with mild or sub-clinical infections. Another important aspect that we are currently addressing is the durability of neutralizing antibody responses in recovered COVID-19 patients.

### STAR METHODS

Detailed methods are provided in the online version of this paper and include the following:

- **KEY RESOURCES TABLE**
- **RESOURCE AVAILABILITY**
  - Lead Contact
  - Materials Availability
  - Data and Code Availability
- **EXPERIMENTAL MODEL AND SUBJECT DETAILS**
  - Ethics statement
  - Virus
  - Cells
- **METHOD DETAILS**
  - Cloning, expression, and purification of SARS-CoV-2 RDB
  - Preparation of CR3022 monoclonal antibody and biotinylation
  - Sequence analysis and alignment
  - ELISA assays
  - Clinical RBD ELISA assay
  - Focus Reduction Neutralization Assays

- **QUANTIFICATION AND STATISTICAL ANALYSIS**
  - Statistical analysis

### SUPPLEMENTAL INFORMATION

Supplemental Information can be found online at <https://doi.org/10.1016/j.xcrm.2020.100040>.

### ACKNOWLEDGMENTS

We would like to thank Laurel Bristow, Ariel Kay, Youssef Saklawi, Ghina Alaaeddine, Nina McNair, Ellie Butler, Brandi Johnson, Christopher Huerta, Jennifer Kleinhenz, Vinit Karmali, Yong Xu, Dongli Wang, and Michele McCullough for sample processing at the Hope Clinic. We also acknowledge the dedicated efforts of Hassan Bilal, DeAndre Brown, Davette Campbell, Lisa Cole, Ginger Crews, Shanessa Fakour, Natalie Hicks, Mark Meyers, and Katherine Normile for sample collection, processing, and organization. We thank Gabrielle Hostenstein, Corin Jones, Alethea Luo-Gardner, Hoa Nguyen, Keyanna Seville, and Corazon Tomblin for the exceptional technical performance of the ELISA at the Emory Medical Laboratories. We also acknowledge thorough and rapid chart reviews by Kari Broder. We thank Guido Silvestri for helpful discussions. We thank Michael Konomos for help with generating the graphical abstract. Finally, we thank all the participating patients and the hospital staff caring for them. This work was funded in part by an Emory EVPHA Synergy Fund award (M.S.S. and J.W.), and by the National Institutes of Health NIAID Infectious Diseases Clinical Research Consortium (IDCRC) UM1 AI148684 (D.S.S., R.A., and J.W.), R01 AI137127 (J.W.), ORIP/OD P51OD011132 (M.S.S.), 5T32 AI074492 (S.L.L.), R00 AG049092 (V.D.M.), World Reference Center for Emerging Viruses and Arboviruses R24 AI120942 (V.D.M.), HIPC 5U19AI090023-10 (N.R., E.A., and A.M.), VTEU 1UM1AI148576-01 (E.A. and N.R.), and a grant from The Marcus Foundation (J.D.R.). The funders had no role in study design, data collection and analysis, decision to publish, or preparation of the manuscript.

### AUTHOR CONTRIBUTIONS

M.S., S.R., H.P.V., D.N.A., J.G., G.M., S.L., and A.V. contributed to the acquisition, analysis, and interpretation of the data, J.B. and M.C.H. contributed to the acquisition and interpretation of the data, C.M.A. and N.S. contributed to the acquisition of the data, G.H.S., M.G.Z., and R.C.K. contributed to the acquisition, analysis, and interpretation of the data and helped draft the work, A.K.M., A.S.N., and S.R.S. contributed to the acquisition, analysis, and interpretation of the data, as well as the conception and design of the work, D.S.S., L.N., S.A., M.A., W.H.H., C.W.D., and V.D.M. contributed to the analysis, and interpretation of the data, S.E. served as the principal investigator of the clinical protocol for acquisition of patient samples and contributed to the interpretation of data, E.M.S., K.H., A.C., J.A.M., N.R., and E.J.A. contributed to the acquisition and interpretation of the data, and J.D.R., R.A., J.W., and M.S.S. contributed to the acquisition, analysis, and interpretation of the data, as well as the conception and design of the work, and writing the manuscript.

### DECLARATION OF INTERESTS

The authors declare no competing interests.

Received: April 29, 2020  
Revised: May 28, 2020  
Accepted: May 29, 2020  
Published: June 5, 2020

### REFERENCES

1. Bolles, M., Donaldson, E., and Baric, R. (2011). SARS-CoV and emergent coronaviruses: viral determinants of interspecies transmission. *Curr. Opin. Virol.* 7, 624–634.

2. Deming, D., Sheahan, T., Heise, M., Yount, B., Davis, N., Sims, A., Suthar, M., Harkema, J., Whitmore, A., Pickles, R., et al. (2006). Vaccine efficacy in senescent mice challenged with recombinant SARS-CoV bearing epidemic and zoonotic spike variants. *PLoS Med.* 3, e525.
3. Buchholz, U.J., Bukreyev, A., Yang, L., Lamirande, E.W., Murphy, B.R., Subbarao, K., and Collins, P.L. (2004). Contributions of the structural proteins of severe acute respiratory syndrome coronavirus to protective immunity. *Proc. Natl. Acad. Sci. USA* 101, 9804–9809.
4. Bosch, B.J., van der Zee, R., de Haan, C.A., and Rottier, P.J. (2003). The coronavirus spike protein is a class I virus fusion protein: structural and functional characterization of the fusion core complex. *J. Virol.* 77, 8801–8811.
5. Hoffmann, M., Kleine-Weber, H., Schroeder, S., Kruger, N., Herrler, T., Erichsen, S., Schiergens, T.S., Herrler, G., Wu, N.H., Nitsche, A., et al. (2020). SARS-CoV-2 Cell Entry Depends on ACE2 and TMPRSS2 and Is Blocked by a Clinically Proven Protease Inhibitor. *Cell* 181, 271–280.
6. Wang, Q., Zhang, Y., Wu, L., Niu, S., Song, C., Zhang, Z., Lu, G., Qiao, C., Hu, Y., Yuen, K.Y., et al. (2020). Structural and Functional Basis of SARS-CoV-2 Entry by Using Human ACE2. *Cell* 181, 894–904.
7. Tortorici, M.A., and Veasley, D. (2019). Structural insights into coronavirus entry. *Adv. Virus Res.* 105, 93–116.
8. Li, F., Li, W., Farzan, M., and Harrison, S.C. (2005). Structure of SARS coronavirus spike receptor-binding domain complexed with receptor. *Science* 309, 1864–1868.
9. Lu, G., Hu, Y., Wang, Q., Qi, J., Gao, F., Li, Y., Zhang, Y., Zhang, W., Yuan, Y., Bao, J., et al. (2013). Molecular basis of binding between novel human coronavirus MERS-CoV and its receptor CD26. *Nature* 500, 227–231.
10. Walls, A.C., Park, Y.J., Tortorici, M.A., Wall, A., McGuire, A.T., and Veasley, D. (2020). Structure, Function, and Antigenicity of the SARS-CoV-2 Spike Glycoprotein. *Cell* 181, 281–292.
11. ter Meulen, J., van den Brink, E.N., Poon, L.L., Marissen, W.E., Leung, C.S., Cox, F., Cheung, C.Y., Bakker, A.Q., Bogaards, J.A., van Deventer, E., et al. (2006). Human monoclonal antibody combination against SARS coronavirus: synergy and coverage of escape mutants. *PLoS Med.* 3, e237.
12. Harcourt, J., Tamin, A., Lu, X., Kamili, S., Sakthivel, S.K., Murray, J., Queen, K., Tao, Y., Paden, C.R., Zhang, J., et al. (2020). Severe Acute Respiratory Syndrome Coronavirus 2 from Patient with Coronavirus Disease, United States. *Emerg. Infect. Dis.* 26, 1266–1273.
13. Rockx, B., Corti, D., Donaldson, E., Sheahan, T., Stadler, K., Lanzavecchia, A., and Baric, R. (2008). Structural basis for potent cross-neutralizing human monoclonal antibody protection against lethal human and zoonotic severe acute respiratory syndrome coronavirus challenge. *J. Virol.* 82, 3220–3235.
14. Lee, Y.L., Liao, C.H., Liu, P.Y., Cheng, C.Y., Chung, M.Y., Liu, C.E., Chang, S.Y., and Hsueh, P.R. (2020). Dynamics of anti-SARS-Cov-2 IgM and IgG antibodies among COVID-19 patients. *J. Infect.* Published online April 23, 2020. <https://doi.org/10.1016/j.jinf.2020.04.019>.
15. Okba, N.M.A., Müller, M.A., Li, W., Wang, C., GeurtsvanKessel, C.H., Cormann, V.M., Lamers, M.M., Sikkema, R.S., de Bruin, E., Chandler, F.D., et al. (2020). Severe Acute Respiratory Syndrome Coronavirus 2-Specific Antibody Responses in Coronavirus Disease 2019 Patients. *Emerg. Infect. Dis.* 26, 9.
16. Bloch, E.M., Shoham, S., Casadevall, A., Sachais, B.S., Shaz, B., Winters, J.L., van Buskirk, C., Grossman, B.J., Joyner, M., Henderson, J.P., et al. (2020). Deployment of convalescent plasma for the prevention and treatment of COVID-19. *J. Clin. Invest.* 130, 2757–2765.
17. Shen, C., Wang, Z., Zhao, F., Yang, Y., Li, J., Yuan, J., Wang, F., Li, D., Yang, M., Xing, L., et al. (2020). Treatment of 5 Critically Ill Patients with COVID-19 with Convalescent Plasma. *JAMA* 323, 1582–1589.
18. Liu, W., Fontanet, A., Zhang, P.H., Zhan, L., Xin, Z.T., Baril, L., Tang, F., Lv, H., and Cao, W.C. (2006). Two-year prospective study of the humoral immune response of patients with severe acute respiratory syndrome. *J. Infect. Dis.* 193, 792–795.
19. Amanat, F., and Krammer, F. (2020). SARS-CoV-2 Vaccines: Status Report. *Immunity* 52, 583–589.
20. Smith, K., Garman, L., Wrammert, J., Zheng, N.Y., Capra, J.D., Ahmed, R., and Wilson, P.C. (2009). Rapid generation of fully human monoclonal antibodies specific to a vaccinating antigen. *Nat. Protoc.* 4, 372–384.
21. Wrapp, D., Wang, N., Corbett, K.S., Goldsmith, J.A., Hsieh, C.L., Abiona, O., Graham, B.S., and McLellan, J.S. (2020). Cryo-EM structure of the 2019-nCoV spike in the prefusion conformation. *Science* 367, 1260–1263.

## STAR METHODS

### KEY RESOURCES TABLE

REAGENT or RESOURCE	SOURCE	IDENTIFIER
<b>Antibodies</b>		
Peroxidase AffiniPure F(ab') <sub>2</sub> Fragment Goat Anti-Human IgM, Fc5 <sub>μ</sub> fragment specific	Jackson ImmunoResearch	Cat# 109-036-129, RRID:AB_2337598
Peroxidase AffiniPure F(ab') <sub>2</sub> Fragment Goat Anti-Human Serum IgA, α chain specific	Jackson ImmunoResearch	Cat# 109-036-011, RRID:AB_2337592
Peroxidase AffiniPure F(ab') <sub>2</sub> Fragment Goat Anti-Human IgG, Fc <sub>γ</sub> fragment specific	Jackson ImmunoResearch	Cat# 109-036-098, RRID:AB_2337596
Mouse Anti- Human IgG1 Fc-HRP	Southern Biotech	Cat# 9054-05, RRID:AB_2796627
Mouse Anti- Human IgG2 Fc-HRP	Southern Biotech	Cat# 9060-05, RRID:AB_2796633
Mouse Anti- Human IgG3 Hinge-HRP	Southern Biotech	Cat# 9210-05, RRID:AB_2796699
Mouse Anti- Human IgG4 Fc-HRP	Southern Biotech	Cat# 9200-05, RRID:AB_2796691
<b>Virus Strains</b>		
2019-nCoV/USA-WA1-A12/2020 (SARS-CoV-2)	CDC, Atlanta, GA	GenBank Accession #MT020880
<b>Biological Samples</b>		
Human Serum/Plasma samples	Emory University Hospital/Emory Medical Laboratories	N/A
<b>Chemicals, Peptides, and Recombinant Proteins</b>		
Recombinant binding protein (SARS-CoV-2 Spike)	Dr. Jens Wrannert Emory University	N/A
Methylcellulose	Sigma-Aldrich	Cat. #: M0512-250G
TrueBlue Peroxidase Substrate	KPL	Cat. #: 5067428
<b>Experimental Models: Cell Lines</b>		
VeroE6 C1008 cells	ATCC	Cat# CRL-1586, RRID:CVCL_0574
<b>Software and Algorithms</b>		
GraphPad Prism (v7 and v8)	N/A	N/A

### RESOURCE AVAILABILITY

#### Lead Contact

Further information and requests for resources and reagents should be directed to and will be fulfilled by the Lead Contact Author Mehul Suthar ([mehul.s.suthar@emory.edu](mailto:mehul.s.suthar@emory.edu)).

#### Materials Availability

All unique/stable reagents generated in this study are available from the Lead Contact with a completed Materials Transfer Agreement.

#### Data and Code Availability

The datasets supporting the current study are available from the corresponding author on request.

### EXPERIMENTAL MODEL AND SUBJECT DETAILS

#### Ethics statement

The serum and plasma samples used for this study were collected at Emory University Hospital and Emory University Hospital Midtown in Atlanta. All patients were adults diagnosed with acute SARS-CoV-2 infection by PCR, and samples were collected at a range of times post-PCR-confirmation. No specific criteria or demographics were used for enrollment beyond PCR confirmed SARS-CoV-2 infection. All collection, processing, and archiving of human specimens was performed under approval from the University Institutional Review Board (IRB #00000510 and #00022371). For IRB #00000510, informed consent was obtained prior to

patient participation. For #00022371, an IRB waiver was obtained allowing the use of discarded samples in the clinical laboratory at the Emory Hospital.

### Virus

SARS-CoV-2 (2019-nCoV/USA\_WA1/2020) was isolated from the first reported case in the US<sup>12</sup>. A plaque purified passage 4 stock was kindly provided by Natalie Thornburg (CDC, Atlanta, GA). Viral titers were determined by plaque assay on Vero cells (ATCC).

### Cells

VeroE6 cells were obtained from ATCC (C1008) and cultured in complete DMEM medium consisting of 1x DMEM (Corning Cellgro), 10% FBS, 25mM HEPES Buffer (Corning Cellgro), 2mM L-glutamine, 1mM sodium pyruvate, 1x Non-essential Amino Acids, and 1x antibiotics. Expi293F cells were obtained from ThermoFisher Scientific (A14527), and maintained according to the manufacturer's protocols.

## METHOD DETAILS

### Cloning, expression, and purification of SARS-CoV-2 RDB

A recombinant form of the spike glycoprotein receptor-binding domain (RBD) from SARS-CoV-2, Wuhan-Hu-1 (GenPept: QHD43416) was cloned for mammalian expression in human embryonic kidney expi293F cells. The receptor-binding domain consisting of amino acids 319 (arginine) to 541 (phenylalanine) of the SARS-Cov-2 S gene was amplified by PCR using a mammalian codon-optimized sequence as the DNA template (Genscript MC\_0101081). PCR amplification appended the first 12 amino acids of the native S gene signal peptide sequence to the N-terminal end of the protein and, at the C-terminal end a 6X polyhistidine tag preceded by a short linker sequence (GGGGS).

Forward and Reverse primer sequences consisted were:

5'-AGAGAAATTCACCATGTTTCGTCTTCCTGGTCTGCTGCCTCTGGTCTCCAGGGTGCAGC CACCGAGTCTATC-3'

and 5'-CTCTAAGCTTCTATCATTAGTGGTGGTGGTGGTGGCTTCCGCCTCCGCCGAA GTTCACGCACCTGTTCTTCAC-3'.

25  $\mu$ L PCR reaction conditions were: 1X Phusion HF Buffer, 0.2 mM dNTP, 0.63 units Phusion DNA polymerase, and 500 nM of each primer. PCR cycling conditions were: initial denaturation at 98°C, 1 minute; then 25 cycles of: 98°C, 20 s, 65°C 30 s, 72°C 30 s; followed a final extension at 72°C for 5 minutes. Following amplification, purified PCR products (QIAquick PCR Purification, QIAGEN) were digested with EcoRI-HF (NEB) and HindIII (NEB) and cloned into the EcoRI-HindIII cloning site of a mammalian expression vector containing a CMV promoter (GenBank Reference ID FJ475055). Plasmid DNA was prepared using the QIAGEN PlasmidPlus Midi purification system and constructs were sequence verified. Recombinant protein expression was performed in Expi293F cells according to the manufacturer's instructions (ThermoFisher Scientific). Briefly, expression plasmid DNA was complexed with the expifectamine lipid-based transfection reagent. Complexes were added to the cell suspensions shaking at 125 RPM and incubated overnight at 37°C in an 8% CO<sub>2</sub> humidified incubator. After 20 hours, protein expression supplements and antibiotics were added. Cultures were then incubated for an additional three days to allow for expression into the supernatant. Cell culture supernatants were harvested by centrifugation at 16,000xg for 10 minutes. Supernatants were sterile filtered through a 0.2  $\mu$ m filter and stored at 4°C for < 7 days before purification. Analytical SDS-PAGE was performed on supernatants and the protein concentration in solution was determined by densitometry relative to the purified protein. Recombinant RBD protein levels were between 100 mg and 150 mg per liter. Purification was performed according to manufacturer's instructions using 5 mL HisTALON Superflow Cartridges (Clontech Laboratories). Briefly, an additional 11.7 g/L of sodium chloride and 0.71 g/L of cobalt(II) chloride hexahydrate were added to culture supernatants, which were adjusted to pH 7.5. The supernatant was then loaded on to the column equilibrated with 10 column volumes of 50 mM phosphate 300 mM sodium chloride buffer pH 7.5 (equilibration buffer). The column was washed with 8 column volumes of equilibration buffer supplemented with 10 mM imidazole. Protein was eluted with 6 column volumes of equilibration buffer supplemented with 150 mM imidazole. The eluted protein was dialyzed overnight against 80 volumes of phosphate-buffered saline pH 7.2. The protein was filter-sterilized (0.2  $\mu$ m) and normalized to 1 mg/mL by UV spectrophotometry using an absorption coefficient of 1.3 AU at 280 nm = 1 mg/mL. Proteins were aliquoted and stored at -80°C prior to use. SDS-PAGE analysis of purified recombinant protein stained with Coomassie blue demonstrated that samples were > 90% pure (Figure 1). The RBD resolves at an apparent molecular weight of 30 kDa (Figure 1D) which is slightly larger than the theoretical molecular weight of 26.5 kDa, presumably caused by glycosylation.

### Preparation of CR3022 monoclonal antibody and biotinylation

The SARS-CoV S glycoprotein specific antibody CR3022 was generated recombinantly using previously reported heavy and light variable domain sequences deposited in GenBank under accession numbers DQ168569 and DQ168570<sup>11</sup>. Antibody variable domain gene sequences were synthesized by IDT and cloned into human IgG1 and human kappa expression vectors as previously described<sup>20</sup>. Antibodies were produced in Expi293F cells according to the manufacturer's recommendations by co-transfecting heavy and light chain plasmids at a ratio of 1:1.5. Antibodies were purified using rProtein A Sepharose Fast Flow antibody purification

resin (GE Healthcare) and buffer exchanged into PBS before use. Biotinylated versions of CR3022 used in viral neutralization assays were produced by combining the antibody with a 20 molar excess of EZ-Link NHS-PEG4-Biotin (ThermoFisher Scientific) for 1 hour at room temperatures. Reactions were stopped by adding Tris pH 8 to a final concentration of 10 mM. The biotinylated antibody was then buffer exchanged > 1000X into PBS using a 10 kDa protein spin-concentrator (Amicon).

### Sequence analysis and alignment

The SARS-CoV-2 spike protein structure<sup>21</sup> was visualized in Pymol (Schrödinger, LLC). To assess the homology of coronavirus spike proteins, a global protein alignment was performed in Geneious (Geneious, Inc.) with translations of genome sequences accessed through NCBI Nucleotide. Sequences used were GenBank MN908947.3 (SARS-CoV-2), RefSeq NC\_004718.3 (SARS-CoV), RefSeq NC\_019843.3 (MERS-CoV), NC\_006577.2 (HCoV-HKU1), RefSeq NC\_006213.1 (HCoV-OC43), RefSeq NC\_005831.2 (HCoV-NL63), and RefSeq NC\_005831.2 (HCoV-229E). Homology at the RBD was determined by sequence identity between SARS-CoV-2 RBD residues T302 to L560<sup>6,10</sup>.

### ELISA assays

Recombinant SARS-CoV-2 RDB was coated on Nunc MaxiSorp plates at a concentration of 1 μg/mL in 100 uL phosphate-buffered saline (PBS) at 4°C overnight. Plates were blocked for two hours at room temperature in PBS/0.05% Tween/1% BSA (ELISA buffer). Serum or plasma samples were heated to 56°C for 30 min, aliquoted, and stored at –20°C before use. Samples were serially diluted 1:3 in dilution buffer (PBS-1% BSA-0.05% Tween-20) starting at a dilution of 1:100. 100 μL of each dilution was added and incubated for 90 minutes at room temperature. 100 uL of horseradish peroxidase-conjugated isotype and subclass specific secondary antibodies, diluted 1 to 2,000 in ELISA buffer, were added and incubated for 60 minutes at room temperature. Development was performed using 0.4 mg/mL o-phenylenediamine substrate (Sigma) in 0.05 M phosphate-citrate buffer pH 5.0, supplemented with 0.012% hydrogen peroxide before use. Reactions were stopped with 1 M HCl and absorbance was measured at 490 nm. Between each step, samples were washed four times with 300 uL of PBS-0.05% Tween. Prior to development, plates were additionally washed once with 300 uL of PBS. Secondary antibodies used for development were as follows: anti-hu-IgM-HRP, anti-hu-IgG-HRP, and anti-hu-IgA-HRP (Jackson Immuno Research, and Mouse anti-hu-IgG1 Fc-HRP, Mouse anti-hu-IgG2 Fc-HRP, Mouse anti-hu-IgG3 Fc-HRP, or Mouse anti-hu-IgG4 Fc-HRP (Southern Biotech).

### Clinical RBD ELISA assay

This assay was performed essentially as described above, with the following modifications to increase throughput: all serum samples were diluted 1:200, and the incubation times were reduced to 30 minutes after the addition of serum samples and the secondary antibody conjugate.

### Focus Reduction Neutralization Assays

Serially diluted patient plasma and COVID-19 (100–200 FFU) were combined in DMEM + 1% FBS (Corning Cellgro), and incubated at 37°C for 1 hour. The antibody-virus mixture was aliquoted on a monolayer of VeroE6 cells, gently rocked to distribute the mixture evenly, and incubated at 37°C for 1 hour. After 1 hour, the antibody-virus inoculum was removed and prewarmed DMEM supplemented with 1% FBS (Optima, Atlanta Biologics), HEPES buffer (Corning Cellgro), 2mM L-glutamine (Corning Cellgro), 1mM sodium pyruvate (Corning Cellgro), 1x Non-essential Amino Acids (Corning Cellgro), 1x antibiotics (penicillin, streptomycin, amphotericin B; Corning Cellgro) was mixed with methylcellulose (DMEM [Corning Cellgro], 1% antibiotic, 2% FBS, 2% methylcellulose [Sigma Aldrich]) at a 1:1 ratio and overlaid on the infected VeroE6 cell layer. Plates were incubated at 37°C for 24 hours. After 24 hours, plates were gently washed three times with 1x PBS (Corning Cellgro) and fixed with 200 μl of 2% paraformaldehyde (Electron Microscopy Sciences) for 30 minutes. Following fixation, plates were washed twice with 1x PBS and 100 μl of permeabilization buffer (0.1% BSA-Saponin in PBS) (Sigma Aldrich), was added to the fixated Vero cell monolayer for 20 minutes. Cells were incubated with an anti-SARS-CoV spike protein primary antibody conjugated to biotin (CR3022-biotin) for 1–2 hours at room temperature, then with avidin-HRP conjugated secondary antibody for 1 hour at room temperature. Foci were visualized using True Blue HRP substrate and imaged on an ELISPOT reader (CTL). Each plate contained three positive neutralization control wells, three negative control wells containing healthy control serum mixed with COVID-19, and three mock-infected wells.

## QUANTIFICATION AND STATISTICAL ANALYSIS

### Statistical analysis

FRNT<sub>50</sub> curves were generated by non-linear regression analysis using the 4PL sigmoidal dose curve equation on Prism 8 (Graphpad Software). Maximum neutralization (100%) was considered the number of foci counted in the wells infected with a virus mixed with COVID-19 naive healthy patient serum. Neutralization titers were calculated as 100% x [1 - (average number of foci in wells incubated with COVID-19 patient serum) ÷ (average number of foci in wells incubated with control serum)]. For the clinical data Receiver Operating Characteristic (ROC) curves were generated separately for each of three cohorts of clinical validation samples with

progressively increasing PCR-to-serum collection intervals (0-3 days, 4-6 days, 7+ days). Optical densities (OD) for each sample were entered into Microsoft Excel for Office 365 v16, and a custom software package was used to iteratively compute the false positive rate (1 - specificity) and true positive rate (sensitivity) at every OD cutoff level for each cohort. The false-positive rates (x) and true positive rates (y) were then rendered as scatterplots to generate the ROC curves. Correlations analyses were done by log transforming RBD binding titers or neutralization titers, followed by linear regression analysis. The  $R^2$  and p value are reported in each figure.